

Supplementary Information

***In situ* ion exchange synthesis of the novel Ag/AgBr/BiOBr hybrid with highly efficient decontamination of pollutants**

Hefeng Cheng, Baibiao Huang*, Peng Wang, Zeyan Wang, Zaizhu Lou, Junpeng
Wang, Xiaoyan Qin, Xiaoyang Zhang and Ying Dai

Experimental Section

Synthesis of BiOBr hierarchical microspheres: In a typical synthetic procedure, Bi(NO₃)₃·5H₂O (2 mmol) and 1-dodecyl-3-methylimidazolium bromide ([C₁₂Mim]Br) (3 mmol) were dissolved in 40 mL of 2-methoxyethanol, respectively, with constant stirring. The two solutions were mixed together and further magnetically stirred for 10 min, and then transferred into a 100 mL Teflon-lined stainless autoclave. The autoclave was heated and maintained at 160 °C for 2 h, and then cooled down to room temperature. The product was collected, washed, and dried in vacuum. For comparison, BiOBr nanoplates were also prepared in ethanol instead of 2-methoxyethanol solvent.

Synthesis of Ag/AgBr/BiOBr composite: The AgBr/BiOBr hybrid composite was prepared by an *in situ* ion-exchange route. BiOBr sample (1 mmol) was dispersed in 80 mL ethylene glycol containing AgNO₃ (0.5 mmol), and vigorously stirred overnight. The obtained AgBr/BiOBr samples were then reduced by light to generate Ag/AgBr/BiOBr products [1].

For comparison, we also prepared Ag/AgBr sample through direct precipitation of AgNO₃ and KBr aqueous solution followed by light reduction. Besides, AgBr/BiOBr sample was also prepared by ion exchange with AgNO₃ aqueous solution and BiOBr nanoplates.

N-doped P25, which was used as the reference photocatalyst, was obtained according to the method previously reported [2].

Characterization: Powder X-ray diffraction (XRD) patterns were recorded on a Bruker AXS D8 advance powder diffractometer (Cu K α X-ray radiation, $\lambda = 0.154056$ nm). X-ray photoelectron spectroscopy (XPS) measurements were carried out on a Thermo Fisher Scientific Escalab 250 spectrometer with monochromatized Al K α excitation, and C 1s (284.6 eV) was used to calibrate the peak positions of the elements. The scanning electron microscopy (SEM) images were obtained on a Hitachi S-4800 microscope with an accelerating voltage of 7.0 kV. UV-vis diffuse reflectance spectra were collected on a Shimadzu UV 2550 recording spectrophotometer, which was equipped with an integrating sphere.

Anti-bacterial activity: The anti-bacterial activities were evaluated by inactivation of E. coli in solution containing the photocatalysts under visible light irradiation. The treated cells were measured and diluted to 10^7 colony-forming units (CFU / mL) concentration. A 300 W Xe arc lamp (PLS-SXE300, Beijing Trusttech Co., Ltd.) was used as the light source and equipped with an ultraviolet cutoff filter to provide visible light ($\lambda \geq 400$ nm). The diluted cell suspension (20 mL) and 60 mg photocatalyst were introduced to the conical beaker with a watch glass cover. During the irradiation process, the suspension was magnetically stirred to maintain the concentration

equilibrium and sampled at the given time intervals. An aliquot of the suspension was immediately diluted with sterile deionized water and uniformly spread onto a nutrient agar plate. After 24 h incubation at 37 °C, the colonies were determined by counting the viable cells.

Photodegradation of MO: The photocatalytic performances of the as-prepared products were evaluated by decomposition of methyl orange (MO) under visible light irradiation at room temperature. A 300 W Xe arc lamp (PLS-SXE300, Beijing Trusttech Co., Ltd.) was used as the light source and equipped with an ultraviolet cutoff filter to provide visible light ($\lambda \geq 400$ nm). The distance between the liquid surface of the suspension and the light source was set about 10 cm. The photodegradation experiments were performed with the sample powder (200 mg) suspended in MO (20 mg L⁻¹, 100 mL) with constant stirring. Prior to irradiation, the suspensions were stirred in the dark for 1 h to insure the adsorption/desorption equilibrium. At the given time intervals, about 5 ml of the suspension was taken for the following analysis after centrifugation. The MO photodegradation were then analyzed at 464 nm as a function of irradiation time on a UV–Vis spectrophotometer (Shimadzu UV 2550).

- [1] P. Wang, B. B. Huang, X. Y. Qin, X. Y. Zhang, Y. Dai, J. Y. Wei and M.-H. Whangbo, *Angew. Chem. Int. Ed.*, 2008, **47**, 7931.
- [2] K. Maeda, Y. Shimodaira, B. Lee, K. Teramura, D. Lu, H. Kobayashi and K. Domen, *J. Phys. Chem. C*, 2007, **111**, 18264.

Band position calculations

For a compound, at the point of zero charge, the valence band (VB) position can be calculated by the following empirical formula [3]:

$$E_{VB} = X - E^e + 0.5Eg \quad (2)$$

where X is the absolute electronegativity of the semiconductor, which is defined as the geometric mean of the absolute electronegativity of the constituent atoms, E^e is the energy of free electrons on the hydrogen scale (ca. 4.5 eV), E_{VB} is the VB edge potential and Eg is the band gap of the semiconductor. The conduction band (CB) position can be deduced by $E_{CB} = E_{VB} - Eg$. Given the equations above, the top of the VB and the bottom of the CB of AgBr are calculated to be 2.304 and -0.296 eV with respect to the normal hydrogen electrode (NHE), respectively. Accordingly, in the case of BiOBr, the VB and CB are estimated to be 3.026 and 0.326 eV, respectively.

The calculated band positions of AgBr and BiOBr are summarized in **Table S1**.

Table S1 Band energy positions of AgBr and BiOBr.

oxide	electronegativity	estimated	calculated	calculated
semiconductors	(X)	E_g (eV)	VB position	CB position
			(eV) vs. NHE	(eV) vs. NHE
AgBr	5.804	2.6	2.304	-0.296
BiOBr	6.176	2.7	3.026	0.326

References:

- [3] Y. Xu and M. A. A. Schoonen, *Am. Mineral.*, 2000, **85**, 543; H. F. Cheng, B. B. Huang, Y. Dai, X. Y. Qin and X. Y. Zhang, *Langmuir*, 2010, **26**, 6618.

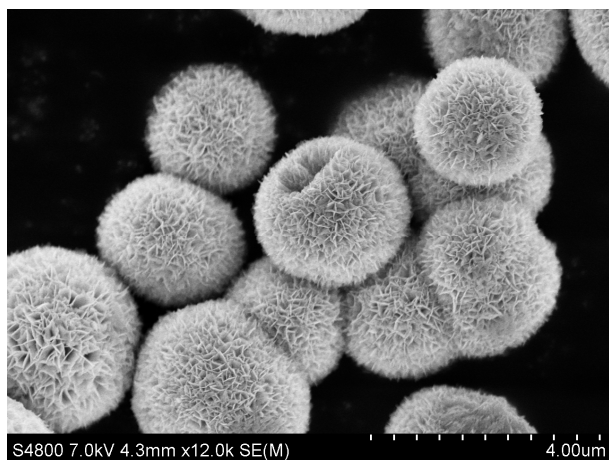


Fig. S1 SEM image of BiOBr hierarchical microspheres.

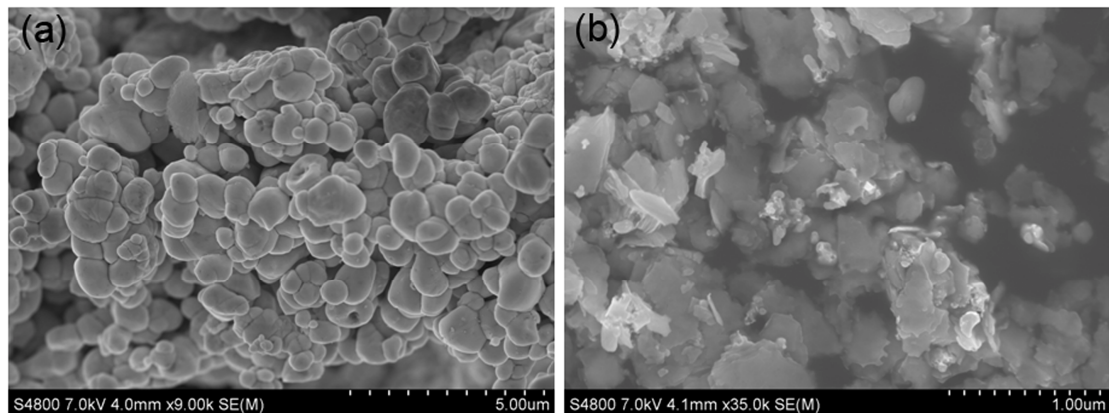


Fig. S2 Typical SEM image of (a)AgBr particles prepared by direct precipitation of AgNO₃ and KBr solution and (b) AgBr particles deposited on BiOBr nanoplates produced by ion exchange with AgNO₃ aqueous solution and BiOBr nanoplates.

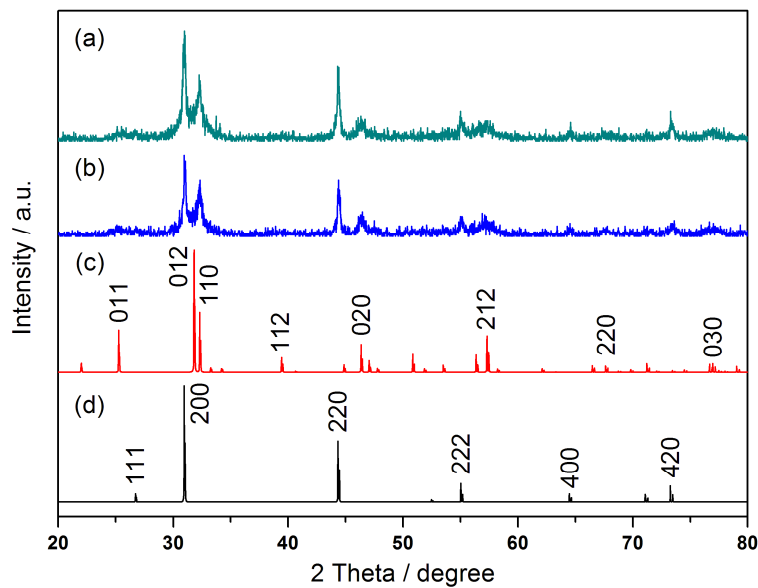


Fig. S3 XRD patterns of (a) fresh Ag/AgBr/BiOBr hybrid, (b) Ag/AgBr/BiOBr hybrid used after five repeated photocatalytic reactions, (c) BiOBr, and (d) AgBr.

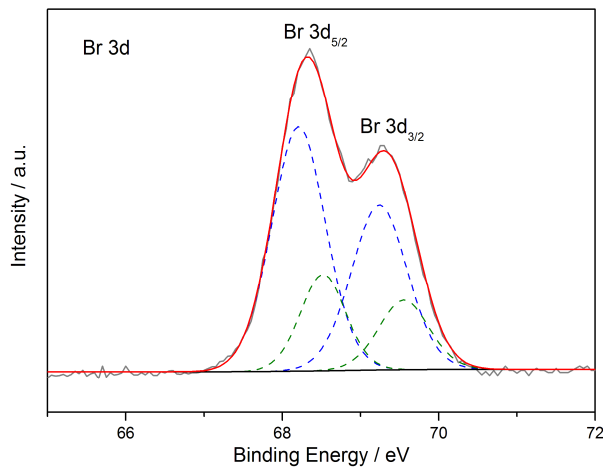


Fig. S4 Br 3d XPS spectra of the fresh Ag/AgBr/BiOBr hybrid.

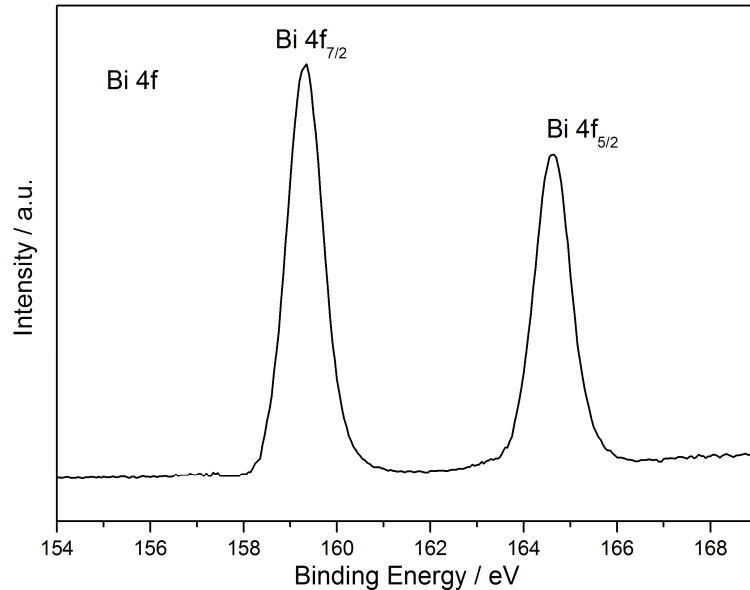


Fig. S5 Bi 4f XPS spectra of the fresh Ag/AgBr/BiOBr hybrid.

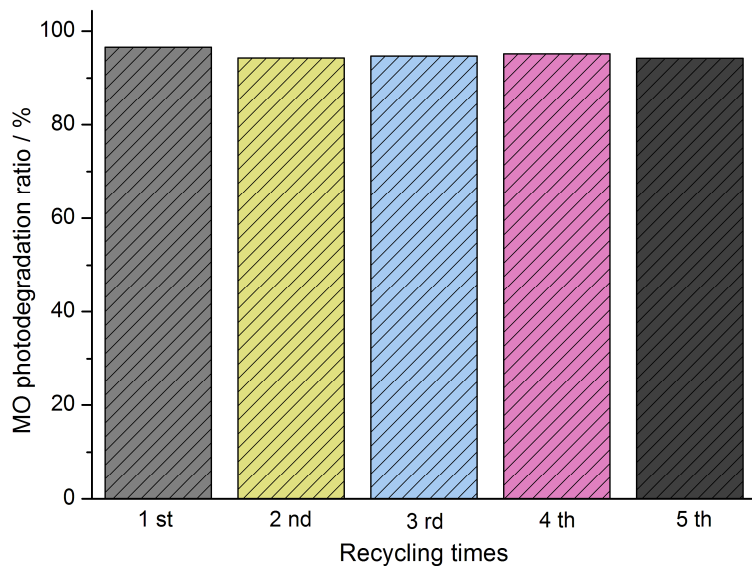


Fig. S6 The repeated MO photodegradation experiments over the Ag/AgBr/BiOBr hybrid under visible light. Each cycle was carried out under visible light for 5 min, which shows no obvious decrease in the photocatalytic efficiency.